THE JOURNAL OF BIOLOGICAL CHEMISTRY Vol. 277, No. 46, Issue of November 15, pp. 44261–44267, 2002
Printed in U.S.A.

Homologues of Human Macrophage Migration Inhibitory Factor from a Parasitic Nematode

GENE CLONING, PROTEIN ACTIVITY, AND CRYSTAL STRUCTURE*

Received for publication, May 13, 2002, and in revised form, September 6, 2002
Published, JBC Papers in Press, September 6, 2002, DOI 10.1074/jbc.M204655200

Xingxing Zang‡§, Paul Taylor¶, Ji Ming Wang‖, David J. Meyer, Alan L. Scott‡‡, Malcolm D. Walkinshaw¶, and Rick M. Maizels‡§§**

*From the ‡Institute of Cell, Animal & Population Biology, University of Edinburgh, Edinburgh EH9 3JT, United Kingdom, ¶Institute of Cell and Molecular Biology, University of Edinburgh, Edinburgh EH9 3JT, United Kingdom, ‖Laboratory of Molecular Immunoregulation, NCI, National Institutes of Health, Frederick Cancer Research and Development Center, Bethesda, Maryland 21702-1201, **Department of Infectious and Tropical Diseases, London School of Hygiene and Tropical Medicine, London WC1E 7HT, United Kingdom, and ‡‡Department of Molecular Microbiology and Immunology, School of Hygiene and Public Health, Johns Hopkins University, Baltimore, Maryland 21205*

Cytokines are the molecular messengers of the vertebrate immune system, coordinating the local and systemic immune responses to infective organisms. We report here functional and structural data on cytokine-like proteins from a eukaryotic pathogen. Two homologues of the human cytokine macrophage migration inhibitory factor (MIF) have been isolated from the parasitic nematode *Brugia malayi*. Both molecules (*Bm*-MIF-1 and *Bm*-MIF-2) show parallel functions to human MIF. They are chemotactic for human monocytes and activate them to produce IL-8, TNF-α, and endogenous MIF. The human and nematode MIF homologues share a tautomerase enzyme activity, which is in each case abolished by the mutation of the N-terminal proline residue. The crystal structure of *Bm*-MIF-2 at 1.8-Å resolution has been determined, revealing a trimeric assembly with an inner pore created by β-stranded sheets from each subunit. Both biological activity and crystal structure reveal remarkable conservation between a human cytokine and its parasite counterpart despite the considerable phylogenetic divide among these organisms. The strength of the similarity implies that MIF-mediated pathways play an important role in nematode immune evasion strategies.

By co-evolving with the immune system, pathogens from viruses to parasites have developed remarkable strategies to circumvent host defenses. Despite the constraints of small genome size, many viruses express multiple gene products that disrupt the normal immunological pathways of recognition and activation (1, 2). For example, effective immunity depends on host cytokines, the secreted proteins that regulate innate and adaptive responses, and viruses produce a spectrum of cytokine-like proteins and cytokine receptor mimics to interfere with normal immune function. Compared with viruses and bacteria, eukaryotic pathogens have much larger genomes, encoding in the case of multicellular helminths of up to 20,000 proteins (3). Moreover, metazoan parasites and their vertebrate hosts share ancestral gene families that have given rise to the modern cytokine genes. Therefore, such parasites have the potential to express a very broad range of immune evasion products including true homologues of mammalian cytokines, but as yet, few examples have been discovered (4, 5).

We have used genomic approaches to identify and characterize homologues of the human cytokine macrophage migration inhibitory factor (MIF)[1] from the parasitic nematode *Brugia malayi*. This parasite is a causative agent of lymphatic filariasis, one of the most important human tropical diseases with an estimated 120 million people infected and an additional 900 million at risk of infection (6). We now report the gene cloning, enzymatic and cellular assay, and crystal structure of a *B. malayi* MIF homologue, demonstrating a functional and three-dimensional structural conservation of a key cytokine between a eukaryotic pathogen and its human host.

EXPERIMENTAL PROCEDURES

Gene Cloning and Protein Expression—Two *B. malayi* expressed sequence tag (EST) clones (GenBank™ accession numbers AA661223 and AA2575777) in the Filarial Genome Project data base (helios.bto.ed.ac.uk/mbx/fgn/filgen.html) were found with similarity to human MIF but with a sequence distinct from a previously described homologue in *B. malayi* now referred to as *Bm*-MIF-1 (4). These EST clones were sequenced and contained the same single open reading frame designated *Bm*-MIF-2. The full-length *Bm*-MIF-2 sequence has been submitted into GenBank under the accession number AY004865. Full-length *Bm*-MIF-1 (U88035) and *Bm*-MIF-2 were subcloned by PCR into pET29 (Novagen, Madison, WI) for expression. Two mutant proteins, *Bm*-MIF-1G (Pro-2 to Gly) and *Bm*-MIF-2G (Pro-2 to Gly), were generated by PCR and subcloned into the same vector. All of the proteins with a C-terminal tag of six histidine residues were overexpressed in *Escherichia coli* strain BL21 (DE3) (Novagen) by induction with isopropyl β-D-thiogalactopyranoside. Proteins were purified to homogeneity on

* This work was supported by grants from the European Commission program for International Co-operation with Developing Countries (INCO-DC, contract IC18.CT970245) and the Wellcome Trust. The costs of publication of this article were defrayed in part by the payment of page charges. This article must therefore be hereby marked "*advertisement*" in accordance with 18 U.S.C. Section 1734 solely to indicate this fact.

The nucleotide sequence(s) reported in this paper has been submitted to the GenBank™/EBI Data Bank with accession number(s) AY004865.

§ Supported by the British Overseas Research Student's Awards. Present address: Howard Hughes Medical Institute, Department of Molecular and Cell Biology, LSA 415, University of California, Berkeley, CA 94720-3200. E-mail: xxzang@uclink4.berkeley.edu.

§§ To whom correspondence should be addressed: Institute of Cell, Animal & Population Biology, University of Edinburgh, Edinburgh EH9 3JT, United Kingdom. Tel.: 44-131-650-5511; Fax: 44-131-650-5450; E-mail: r.maizels@ed.ac.uk.

[1] The abbreviations used are: MIF, macrophage migration inhibitory factor; EST, expressed sequence tag; RT, reverse transcription; *Bm*-MIF, *B. malayi* macrophage migration inhibitory factor; Mf, microfilarial; IL, interleukin; TNF-α, tumor necrosis factor α; RANTES, regulated on activation normal T cell expressed and secreted; JAB1, Jun activation domain-binding protein 1.

HisBind nickel affinity columns (Novagen) from cell lysates. For biological assays, endotoxin was removed from recombinant protein solutions (7) and was determined to be lipopolysaccharide-free by a limulus amebocytelysate gel-clot assay (E-Toxate, Sigma). N-terminal sequencing was performed by Welmet Protein Characterization Facility (University of Edinburgh, Edinburgh, United Kingdom). The purification of human MIF was described previously (8).

Reverse Transcription (RT)-PCR—RNA was extracted using STAT-60 (Biogenesis) from *B. malayi* L3, microfilarial (Mf), and adult worms. Two micrograms of total RNA were used in cDNA synthesis with an oligo(dT) primer and a GeneAmp RNA PCR kit (PerkinElmer Life Sciences). Five percent of each cDNA pool was used as a template for PCR with *Bm*-MIF-2 specific primers matching nucleotides 57–78 (5′-CAATGTTCAGTTTACGGAATTA-3′) and nucleotides 288–70 (5′-GATACAATGCGCTGGATCG-3′) to amplify a 232-bp fragment of *Bm*-MIF-2 cDNA. Thirty cycles of amplification were performed under the following conditions: 94 °C for 1 min, 55 °C for 1 min, and 72 °C for 1 min. PCR products of 232 bp were confirmed by sequencing. Control amplification with primers specific for the *Bm-tph-1* (9) gene under the same conditions indicated that similar amounts of cDNA were present in all samples. Human monocytes purified by monocyte isolation kit (MACS) at 0.5×10^6/ml were incubated with each protein (*Bm*-MIF-1, *Bm*-MIF-1G, *Bm*-MIF-2 and *Bm*-MIF-2G) or medium alone for 16 h in serum-free macrophage (SFM) medium (Invitrogen). RNA preparation and reverse transcription were performed as described above. Five percent of each cDNA pool was used as a template in PCR reaction with human cytokine specific primers for IL-1β, IL-6, IL-8, IL-10, IL-12 (p40), interferon-γ, macrophage inhibitory cytokine, MIF, macrophage inflammatory protein-1, tumor necrosis factor-α (TNF-α), transforming growth factor-β1, and primers for β-actin. PCR was performed as described above.

Western Blotting and Enzyme-linked Immunosorbent Assay—Protein extracts of parasites and excretory-secretory products from adults were made as described previously (10). Proteins were separated on 18% SDS-polyacrylamide gels, and Western blots used mouse polyclonal anti-recombinant *Bm*-MIF-2 and peroxidase-conjugated anti-mouse IgG (Dako) developed with chemiluminescent ECL Plus reagent (Amersham Biosciences). ImageQuant (Amersham Biosciences) was used for analysis of *Bm*-MIF-2 concentration in Western blots. Human monocytes were incubated with *Bm*-MIF-1, *Bm*-MIF-1G, *Bm*-MIF-2, *Bm*-MIF-2G, or medium alone for 16 h in serum-free macrophage medium. TNF-α and IL-8 in supernatants were measured by OPT-EIA kits (BD Biosciences), and MIF was determined by an EIA kit (Chemicon, Temecula, CA).

Assays of Chemotactic Activity and Calcium Mobilization—The chemotaxis assays were performed in a 48-well microchemotaxis chamber (Neuroprobe, Cabin John, MA) (11). Each protein (*Bm*-MIF-1, *Bm*-MIF-1G, *Bm*-MIF-2, and *Bm*-MIF-2G) or medium alone was added to the lower compartment of chemotaxis chambers, and human monocytes were added to the upper compartment, which was separated from the lower compartment by a polycarbonate filters (5-μm pore size, Osmonics, Livermore, CA). After incubation at 37 °C for 90 min, the filter was stained with DiffQuik, and the cells migrated across the filter were counted in high power fields. Intracellular calcium mobilization was measured in human monocytes loaded with 5 mM Fura-2/AM (Molecular Probes, Eugene, OR) for 30 min at room temperature. The dye-loaded cells were washed and resuspended in saline buffer (138 mM NaCl, 6 mM KCl, 1 mM $CaCl_2$, 10 mM HEPES, 5 mM glucose, 0.1% bovine serum albumin, pH 7.4) or Hanks' balanced salt solution at a density of 1×10^6/ml. The cells were then transferred into quartz cuvettes in a luminescence spectrometer (LS-50B, PerkinElmer Life Sciences). Stimulants at different concentrations were added in a volume of 20 μl to each cuvette. The ratio of fluorescence at 340 and 380 nm was recorded over 100 s using a FL WinLab program (PerkinElmer Life Sciences).

Crystallization and Data Collection—Purified *Bm*-MIF-2 was concentrated to 15 mg/ml in a buffer containing 150 mM NaCl, 20 mM Tris-HCl, pH 7.5, for crystallization in a hanging drop by vapor diffusion. Crystals of *Bm*-MIF-2 appeared by mixing protein solution with crystallization buffer containing 1.83 M ammonium sulfate, 0.1 M HEPES buffer, pH 7.5. Heavy atom derivatives were prepared by soaking the crystals in the heavy metal reagents ($HgCl_2$ or $KAu(CN)_2$) at concentrations of 10–30 mM for 1–3 days. Initial data were collected on a Mar image plate using a Nonius FR571 rotating anode and Cu K_α radiation. Data of 243,849 were collected to a resolution of 2.0 Å with a R_{merge} of 5.9%. Datasets of silver and gold heavy metal derivatives were also collected (both to resolution 2.5 Å, R_{merge} 8.7 and 10.1%, respectively).

Structure Determination—Data were processed using Denzo (12). Three datasets were used with the programs Solve (13) and DM (14) to produce a clear envelope of electron density in the spacegroup P31 showing the structure of the trimer. Similar calculations in P3 gave no such clear picture of the electron density. The crystal used for the initial data collection was then used to collect a synchrotron dataset at Daresbury station 9.6 (λ = 0.87 Å) using an ADSC quantum 4 detector to a resolution of 1.8 Å. A total of 398,154 reflections were collected, yielding a dataset with 33,897 unique observations (dataset 98.1% complete with R_{merge} of 4.8%). This dataset was used to perform molecular replacement using the Protein Data Bank code entry 1MIF as a search model. Side chains were then modified to fit the sequence of *Bm*-MIF-2 and to fit the observed electron density[2] WITNOTP Novartis A.G., Basel, Switzerland). G. M. Refinement of the structure was carried out using the program SHELX-97 (G. M. Sheldrick, University of Goettingen, Goettingen, Germany, available at shelx.uni-ac.gwdg.de/SHELX/) with water molecules being added as they appeared in subsequent difference electron density maps. The final structure consists of three chains going from Pro-2 to Met-118 and 241 water molecules. The structure has an *R* factor of 23.27% and an R_{free} of 30.33%.

RESULTS

Identification and Cloning of Bm-mif-2 Gene—To date, the Filarial Genome Project has submitted over 20,000 *B. malayi* ESTs representing more than 8,000 different genes (15). Using protein sequences of human cytokines and their receptors to search this data base, we identified two homologues of the human cytokine MIF from *B. malayi*, one of which was recently reported as *Bm-mif* (4). The second homologue was novel and represented in two ESTs. We designated this new homologue as *Bm-mif-2* and the previously described one as *Bm-mif-1*. From archived EST clones, we isolated full-length *Bm-mif-2* cDNA and determined that it encodes a 120-amino acid polypeptide with a predicted molecular mass of 13.1 kDa (Fig. 1*A*). The protein sequence of *Bm*-MIF-2 shares a 27% identity with human MIF and a 26% identity with *Bm*-MIF-1.

We compared a total of 19 MIF genes for which full open reading frame sequences are currently available in accessible databases and found that six residues are invariant within all 19 members. These six residues are conserved in *Bm*-MIF-1 and *Bm*-MIF-2 (Fig. 1*A*). Interestingly, by searching EST databases, we have also found that MIF homologues are expressed in a range of nematode parasites (data not shown), and further examples have recently been described in both parasitic (16) and free-living species (17).

Expression Pattern of Bm-MIF-2—To investigate the expression of *Bm-mif-2*, we first performed RT-PCR and found *Bm-mif-2* mRNA in all stages of the parasite life cycle. Notably, the relative levels of transcription in lymphatic-dwelling adult worms were higher than in mosquito-born infective larvae (L3) or bloodstream Mf stages (Fig. 1*B*). Western blot analyses with a polyclonal antibody specific for *Bm*-MIF-2 then demonstrated the presence of the 13.1-kDa *Bm*-MIF-2 protein in all stages of the life cycle (Fig. 1*C*). Molecular Dynamics ImageQuant analysis revealed that levels in the long-lived adult parasites were at least 3-fold higher than in Mf stage and 10-fold higher than in the L3 stage, suggesting that *Bm*-MIF-2 is most highly expressed in the adult parasites, which can survive for long periods ($\geq$10 years).

In addition to anatomical and physical defenses such as size, motility, and the presence of a cuticle, the tissue-dwelling parasitic nematode *Brugia* produces and releases as excretory-secretory products a number of molecules that have been implicated in immune interference and evasion (4, 5, 18–22). Therefore, we determined whether *Bm*-MIF-2 is secreted from parasites. Western blot analysis of the supernatant from parasites incubated in serum-free medium for up to 42 h revealed that like mammalian MIF (23) and *Bm*-MIF-1 (4), *Bm*-MIF-2 is

[2] A. Widmer, unpublished data.

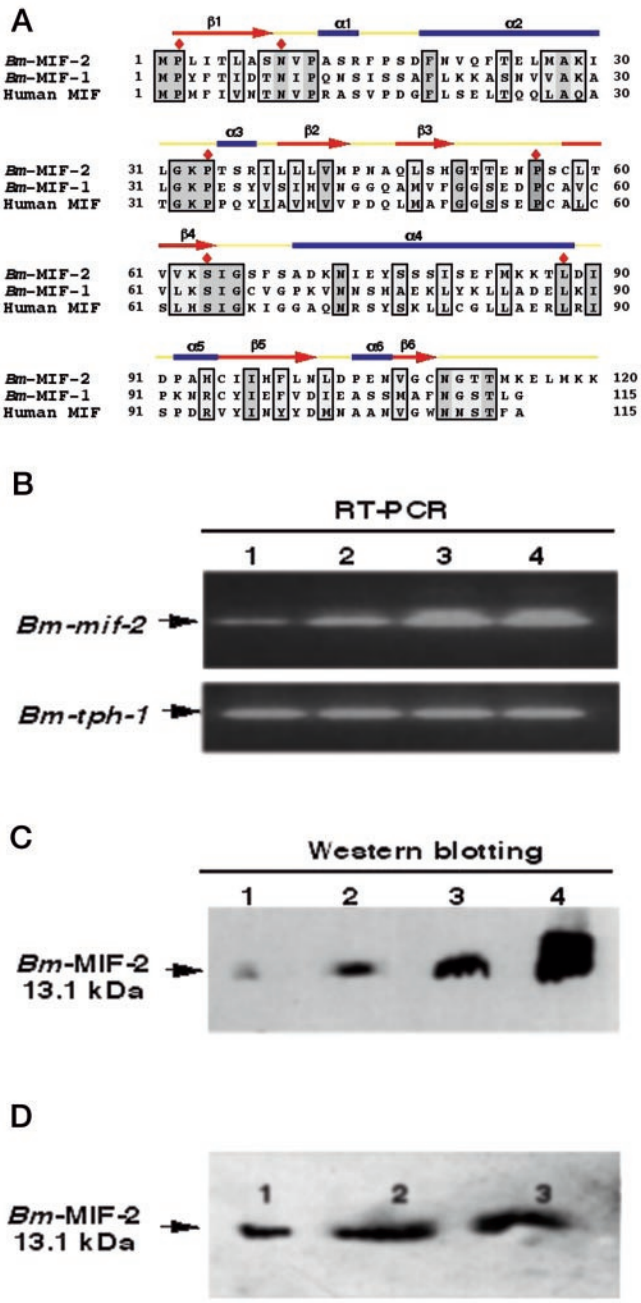

FIG. 1. ***Bm*-MIF-2 is a novel homologue of human MIF and a secreted molecule from the filarial parasite *B. malayi*.** *A*, amino acid sequence of *Bm*-MIF-2 and alignment with MIF family members. Residues that are *highlighted* in *black* show identity, conserved residues are *highlighted* in *gray*, and six residues depicted with *diamonds* are invariant across the whole MIF family. *Red arrows* (labeled β_1–β_4) and *blue bars* (labeled α_1–α_6), respectively, represent β-strands and α-helices in the *Bm*-MIF-2 crystal structure (see Fig. 3). *B*, expression pattern of *Bm-mif-2* mRNA. RT-PCR was performed using a pair of *Bm-mif-2* gene-specific primers and first-strand cDNA converted from poly(A)$^+$ RNA that was obtained from *B. malayi* infective L3 larvae (*lane 1*), Mf (*lane 2*), adult males (*lane 3*), and adult females (*lane 4*) for PCR amplification of a 232-bp fragment (*upper lanes*). As the control, a 425-bp fragment of the constitutively expressed gene *Bm-tph-1* was amplified (*lower lanes*). *C*, expression of *Bm*-MIF-2 protein. For Western blotting, protein extracts from L3 (*lane 1*), Mf (*lane 2*), and mixed adults (*lane 3*) were made: 15 μg of each extract and 1 μg of recombinant *Bm*-MIF-2 (*lane 4*) were separated on 18% SDS-polyacrylamide gels, transferred, and probed with mouse polyclonal antibodies against recombinant *Bm*-MIF-2 by standard chemiluminescence immunoblot procedures. The anti- *Bm*-MIF-2 does not cross-react with *Bm*-MIF-1. *D*, secretion of *Bm*-MIF-2. Mouse polyclonal antibodies to recombinant *Bm*-MIF-2 were used for protein immunoblot analysis. After incubation of the *B. malayi* adults in serum-free RPMI 1640 medium for 24, 36, and 48 h (*lanes 1–3*, respectively), supernatants were concentrated 300-fold and the same volume of samples was then loaded for immunoblot analysis.

a secreted molecule, the amount of secreted *Bm*-MIF-2 increasing with incubation time (Fig. 1*D*). We have also determined that human patients infected with *B. malayi* have a high frequency of serum antibodies to *Brugia* MIF proteins, indicating that they are produced *in vivo*.[3] Most interestingly, the levels of antibodies are highest in uninfected residents of endemic areas, suggesting that immune recognition of *Brugia* MIF-1 and -2 may be linked to protection against infection.

Tautomerase Activity of Brugia MIFs—The initiating Met of mammalian MIF is known to be removed, revealing an N-terminal proline (Pro-2) (23). We determined by N-terminal sequencing that the initiating Met of recombinant *Brugia* MIF is similarly removed. MIF is unique among cytokines in that it enzymatically converts small aromatic substrates such as dopachrome and phenylpyruvate from keto to enol forms (24), a tautomerase activity for which the N-terminal proline acts as the catalytic base (25). We find that this residue is invariant within all 19 members of the MIF family across a broad evolutionary spectrum, supporting the contention that Pro-2 is an essential residue for MIF tautomerase activity. To address the hypothesis that *Brugia* MIFs may display a similar functional activity to the mammalian proteins, *Bm*-MIF-1 and *Bm*-MIF-2 were expressed as recombinant proteins together with site-directed mutants (*Bm*-MIF-1G and *Bm*-MIF-2G) in which Pro-2 of each product was substituted with Gly.

We first investigated tautomerase activity of *Brugia* MIFs and human MIF on a set of related substrates (Table I) (26). Each homologue was active in tautomerizing L-dopachrome methyl ester, phenylpyruvate, and *p*-hydroxyphenylpyruvate but not L-dopachrome. A more subtle difference to emerge was that *Bm*-MIF-2 showed much higher activity with phenylpyruvate as substrate, whereas human MIF showed higher activity toward L-dopachrome methyl ester. The mutants *Bm*-MIF-1G and *Bm*-MIF-2G showed no detectable catalytic activity. These data indicate that, as in mammalian MIF (25), Pro-2 is required for the enzyme activity of *Brugia* MIF-1 and -2.

Chemotactic Activity of Brugia MIF-1 and -2 for Human Monocytes—Given that a major target of mammalian MIF is the macrophage, a key cell in immune and inflammatory responses, we investigated whether *Brugia* MIFs could induce human monocyte migration, a crucial step for cell homing and accumulation. As shown in Fig 2*A*, human monocytes migrated in a dose-dependent manner in response to a concentration gradient of lipopolysaccharide-free recombinant *Bm*-MIF-1 and *Bm*-MIF-2. Concentrations as low as 20 nM *Brugia* MIFs were sufficient for chemotactic activity. These results demonstrate that *Brugia* MIF-1 and -2 can chemotactically mobilize macrophages in manner qualitatively similar to human MIF. The mutant recombinant proteins, *Bm*-MIF-1G and *Bm*-MIF-2G, demonstrated a 10-fold reduction in chemotactic activity for human monocytes (Fig. 2*A*). This is analogous to data showing that although the mutation of Pro-2 in human MIF abolishes all catalytic activity, a residual level of cytokine activity remains in molecules mutated at Pro-2 (25).

No receptor for MIF has yet been described, and so to confirm the functional activity of *Brugia* MIF-1 and -2 on mammalian macrophages, we chose to assay intracellular Ca^{2+} mobiliza-

[3] X. Zang and R. M. Maizels, unpublished observations.

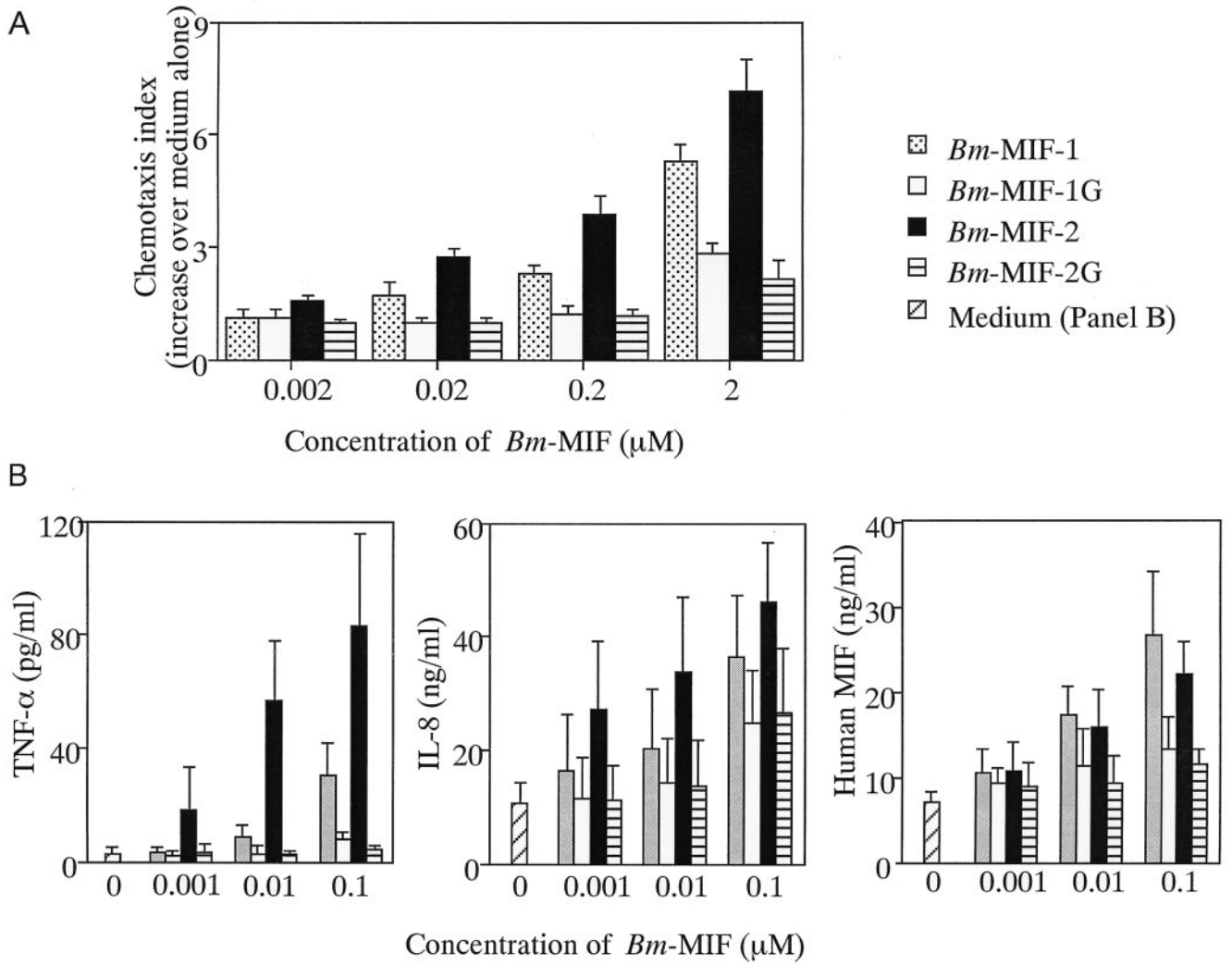

FIG. 2. **Functional effects of *Brugia* MIF-1 and -2 on human monocytes.** *A*, chemotactic activity of *Brugia* MIF-1 and -2. Chemotaxis assays were performed in a 48-well microchemotaxis chamber. Each protein (*Bm*-MIF-1, *Bm*-MIF-1G, *Bm*-MIF-2, and *Bm*-MIF-2G) or medium alone was added to the lower compartment of chemotaxis chambers, and human monocytes were added to the upper compartment, separated from the lower compartment by a polycarbonate filter. After incubation, the filter was stained, and the cells migrated across the filter were counted in high power fields. The experiments were performed five times with each protein, and the results are presented as chemotaxis indices representing the fold increase in the number of migrating cells in response to proteins over the spontaneous cell migration in the presence of control medium. *Error bar*s correspond to the mean ± S.D. of five determinations. *B*, cytokine production of monocytes induced by *Brugia* MIF-1 and MIF–2. Human monocytes were incubated with *Bm*-MIF-1, *Bm*-MIF-1G, *Bm*-MIF-2, *Bm*-MIF-2G, or medium alone for 16 h. TNF-α, IL-8, and human MIF in supernatants were measured. The experiments were performed using monocytes from six different individuals, and *error bars* correspond to means ± S.D. of the six determinations.

tion in human macrophages as an indirect measure of ligation by these homologues. Both *Bm*-MIF-1 and *Bm*-MIF-2 induced Ca^{2+} flux in human monocytes at concentrations of 400 nM-4 μM. In primary cells, cross-desensitization of Ca^{2+} transients is often attributed to two agonists acting on the same receptor. However, *Bm*-MIF-1 and *Bm*-MIF-2 did not desensitize the Ca^{2+} flux in monocytes induced by chemokines such as monocyte chemoattractant protein, macrophage inflammatory protein-1α, and RANTES (regulated on activation normal T cell expressed and secreted). Therefore, the *Brugia* MIF homologues do not share a receptor with any of these chemokines. More recently, JAB1 (Jun activation domain-binding protein 1), a co-activator of the c-Jun transcription factor, has been identified as MIF-binding protein in human cells (27). Interestingly, both *Bm*-MIF-1 and *Bm*-MIF-2 do ligate to the intracellular protein JAB1,[4] indicating that their mode of action closely mimics that of mammalian MIF.

Brugia MIFs Induce Production of IL-8, TNF-α, and Endogenous MIF—Macrophages may adopt contrasting phenotypes depending upon their environment and exposure to cytokines and other stimuli (28, 29). To gain further insight into the functional effect of *Brugia* MIF-1 and -2 on macrophages, we studied the expression of 12 defined cytokines in human monocytes stimulated with *Brugia* MIFs. RT-PCR analysis revealed that stimulation with *Bm*-MIF-1 and *Bm*-MIF-2 resulted in increased TNF-α and IL-8 expression. A number of other cytokine genes such as IL-1β, IL-6, IL-10, IL-12(p40), interferon-γ, monocyte chemoattractant protein-1, macrophage inhibitory cytokine-1, and macrophage inflammatory protein-1α remained unaffected. Therefore, we measured the amounts of TNF-α and IL-8 produced by monocytes after stimulation with *Brugia* MIFs (Fig. 2*B*), confirming this pattern of induction. The mutant proteins again showed approximately a 10-fold less potency in their effect (Fig. 2*B*). Moreover, *Brugia* MIF also induced human MIF production (Fig. 2*B*), demonstrating that *Brugia* MIF-1 and -2 not only stimulate TNF-α and IL-8 pro-

[4] J. Bernhagen, personal communication.

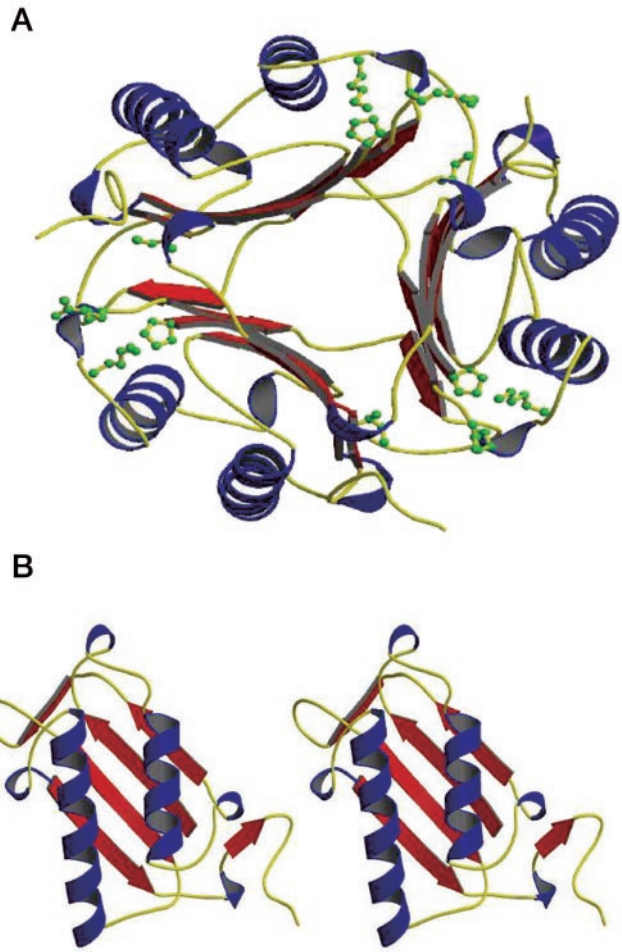

FIG. 3. **Structure of *Bm*-MIF-2 monomer and trimer.** *A*, stereoview of the *Bm*-MIF-2 trimer. Helices are shown in *blue*, and strands are shown in *red*. The side chains of four key residues in the active site are shown: Pro-2, Lys-33, Arg-37, and His-98. *B*, stereoview of the *Bm*-MIF-2 monomer perpendicular to the plane of Fig. 3*A*. The outlying β_3 and β_6 strands form close associations with the neighboring monomers as seen in Fig. 3*A*.

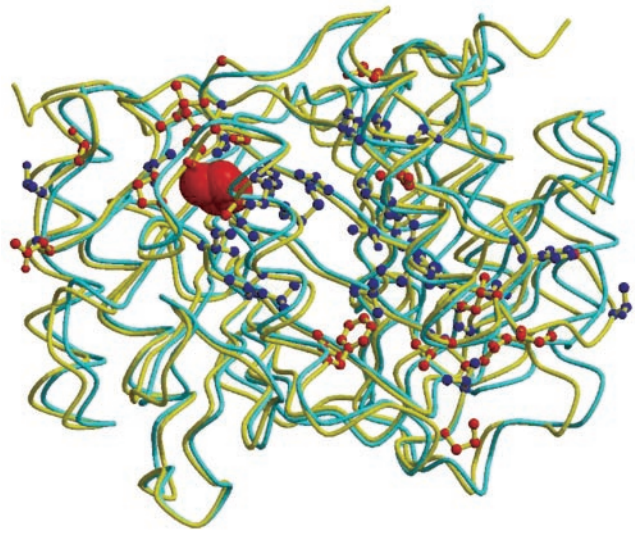

FIG. 4. **Conservation of structure between *Bm*-MIF-2 and human MIF.** Stereoview of backbone trace of *Bm*-MIF-2 (*yellow*) overlaid with human MIF (*cyan*). On one monomer of the *Bm*-MIF-2 molecule, side chains are shown as *red* where identical to human MIF and *blue* where conserved. Pro-2 is shown with a *red* CPK representation of its side chain.

duction as does human MIF (30) but also create a positive feedback by inducing the release of endogenous MIF from host monocytes.

Crystal Structures of Bm-MIF-2—To understand at a molecular level the relationship between human and parasite MIF, we have determined the crystal structure of *Bm*-MIF-2 at 1.8-Å resolution. *Bm*-MIF-2 was found to retain profound structural similarity to human MIF despite sharing only a 27% amino acid identity. *Bm*-MIF-2 forms a trimer with three sheets of β-strands forming around an inner pore (Fig. 3*A*). As with human MIF (31), each sheet is composed of four strands from one monomer together with an additional flanking strand from each of the other two monomers. External to these strands are two major α-helices in each monomer. The root mean square deviation of the backbone C, Cα, and N atoms in the sequence T5-L100 between *Bm*-MIF-2 and human MIF is 0.959 Å. No major differences were observed in the folding of the protein, and in most cases, the changes in side chain were clearly visible in the electron density of *Bm*-MIF-2. An additional three C-terminal residues could also be identified in the first difference map.

The *Bm*-MIF-2 monomer structure (Fig. 3*B*) is characteristic of mammalian MIF (31, 32). An overlay of the human and *Brugia* folds can be seen in Fig. 4, also showing the location of identical and conserved residues. The structures have been aligned using the A monomers of each structure, and it can be seen that other monomers of the trimer are not so well aligned. In *Bm*-MIF-2, the packing environment of each of the monomers is different, leading to some changes in side chain conformation. Thus, the γS of C109 is disordered in two of the monomers but not in the third.

The active site for tautomerase enzyme activity of human MIF has been defined around Pro-2 as a catalytic residue. The substrate also interacts with residues Lys-33, Ile-65, Tyr-96′, and Asn-98′ in which the latter two are contributed by the neighboring monomer (33, 34). Although Pro-2, Lys-33, and Ile-65 are all perfectly conserved in *Bm*-MIF-1 and *Bm*-MIF -2, a Y96′I change is seen in *Bm*-MIF-2, whereas Asn-98′ is altered in both *Brugia* molecules to Glu and His, respectively. Because both *Brugia* MIF-1 and -2 retain strong tautomerase activity, neither Tyr-96 nor Asn-98 appears to be essential for enzymatic function. N98′ (in human MIF) and H98′ (in *Bm*-MIF-2) fulfill in our model the equivalent functions in hydrogen bonding to the phenyl ring of hydroxyphenylpyruvate, whereas another non-conservative substitution (Y37R) is observed without loss of hydrogen bonding to the pyruvate chain of the substrate. Thus, the substitutions at 37 and 98′ are consistent with maintenance of enzyme activity (Table I). However, the aperture leading to the active site proline is changed in *Bm*-MIF-2 in which no less than four neighboring aromatic residues are altered (Y37R, W109C, F114M, and Y96′I). Of these, the most significant may be Y96′I, which enlarges the catalytic pocket significantly. We suggest that this accounts for an increased substrate turnover and the enhanced tautomerization of phenylpyruvate and *p*-hydroxyphenylpyruvate by *Bm*-MIF-2 (Table I).

DISCUSSION

Eukaryotic pathogens such as helminths are not equipped to outpace the immune system by faster cell division or rapid antigenic variation (35). Rather, their strategy appears to be assimilation, defusing aggressive immune reactions, and inducing forms of immunological tolerance to permit their long term survival (18, 36). This feat requires them to override the normal rules of the immune system, which is capable of rejection of tissue expressing even single amino acid changes in

TABLE I
Tautomerase activities of Brugia MIF-1 and MIF-2 and their mutants compared with those of human MIF

The experiments were performed at least five times with each protein, and the results are presented as the average and mean ± S.D. of the five determinations.

Substrate	MIF	Specific activity
		μmol/min/mg
L-Dopachrome	*Bm*-MIF-1	None
	Bm-MIF-1G	None
	Bm-MIF-2	None
	Bm-MIF-2G	None
	Human MIF	None
L-Dopachrome methyl ester	*Bm*-MIF-1	361.3 ± 34.7
	Bm-MIF-1G	None
	Bm-MIF-2	169.4 ± 11.1
	Bm-MIF-2G	None
	Human MIF	529.8 ± 39.2
Phenylpyruvate	*Bm*-MIF-1	1500.7 ± 101.1
	Bm-MIF-1G	3.2 ± 0.2
	Bm-MIF-2	46237.1 ± 3588.2
	Bm-MIF-2G	None
	Human MIF	642.4 ± 46.0
p-Hydroxyphenylpyruvate	*Bm*-MIF-1	106.8 ± 7.7
	Bm-MIF-1G	None
	Bm-MIF-2	517.2 ± 12.5
	Bm-MIF-2G	None
	Human MIF	185.7 ± 13.9

antigenic profile. Eukaryotic pathogens share an extensive genetic ancestry with vertebrates and may have evolved cytokine-like molecules in parallel with their hosts. Here we report the identification, gene cloning, function, and crystal structure of novel members of the MIF family from the parasitic nematode *B. malayi*, showing sophisticated molecular cross-talk occurring between eukaryotic pathogens and human immune system.

MIF is a major immunological mediator with many enigmatic properties (37–39). Despite having been the first cytokine discovered (40, 41), no surface receptor has yet been found for MIF, although binding to an intracellular factor has now been established (27). Furthermore, MIF expression is not restricted to the immune system and is evident in many non-hematopoietic tissues such as the brain (42) and pituitary gland (23). Curiously, MIF has no signal sequence but is readily secreted by transfected cells, implicating a novel pathway of secretion (43). It is also the only cytokine to also possess enzymatic activity despite being <120 amino acids in length, and no physiological substrate has yet been identified for this catalytic activity (44). Thus, both the mode of action and the full biological role of MIF remain to be established.

Originally named for its inhibition of mononuclear cell migration *in vitro*, localizing macrophages to sites of delayed-type hypersensitivity reactions, MIF is now recognized as a pivotal proinflammatory mediator in systemic reactions such as those induced by bacterial endotoxins (23, 45–47). Our results demonstrate striking conservation of both structure and function between parasite and human MIF, a protein intimately associated with the control of inflammation. This presents a paradox because filarial infection induces a suppressed counter-inflammatory phenotype in both humans and mice (48, 49).

The recent discovery that MIF acts within target cells by inactivating JAB1 (27) reveals a contrasting anti-inflammatory pathway that ablates JAB1-dependent cell division and enhancement of AP-1 transcriptional activation. Thus, MIF may promote or counteract inflammation under different circumstances with higher concentrations most likely to block proinflammatory gene expression (38). The occurrence of MIF homologues in a tissue parasite with an anti-inflammatory phenotype may help shed further light on this relationship. We suggest that the parasite is playing a dangerous game by producing a mediator that could induce a lethal attack, but if released in sufficient quantities over time, it can defuse a vital weapon in the host armory. It is interesting also to speculate whether the chronic inflammatory condition suffered by a minority of filariasis patients with sequelae such as lymphedema and elephantiasis are a result of the failure of this gamble by the filarial parasites. Such a hypothesis might also explain the generation of "alternatively activated macrophages" induced by filarial infections, which develop an anti-inflammatory phenotype with properties such as profound suppression of lymphocyte proliferation (29, 50). Supporting this hypothesis, we recently noted that these macrophages express a novel gene that can also be induced *in vivo* by *Brugia* MIF-1 if injected repeatedly over several weeks (51).

Parasites are often long-lived and inhabit immunocompetent hosts for prolonged periods. Consequently, it is not surprising that they should possess modulatory molecules that mitigate host responses to enhance their survival. Some of these modulators act to inhibit initial events such as lymphocyte activation and antigen presentation (20, 52), and others defend parasites from immune effector mechanisms such as the oxidative burst (53, 54). Arguably, the most effective strategy selected by parasites, however, is to interfere with the host cytokine network, thereby regulating multiple cell subsets in a sustained and systemic fashion. Current experiments in our laboratory are aimed at continuous expression of *Brugia* MIF-1 and -2 *in vivo* to ascertain whether the host immune response is indeed redirected in this manner.

MIF homologues can be found in EST databases derived from a range of nematode parasites (data not shown). The presence of MIF in nematodes indicates that MIF has been conserved over ~1 billion years of evolution (55), representing a highly conserved family of genes involved in intercellular communication. Therefore, eukaryotic pathogens may contrast sharply to viruses, which appear to have captured cytokine-like genes from their host species. We suggest instead that the presence of ancestrally related genes in evolving nematodes give these parasites the opportunity to target the host cytokine network for mimicry and disruption to maximize their success. It is interesting to note that recent studies show that MIF also contributes to multiple aspects of tumor progression and neoplasia (56). These data suggest that a possible common strategy between parasites and tumors is the production of MIF to counteract immune activation. In conclusion, the discovery of pathogen MIF will provide dramatic new insights not only into how eukaryotic pathogens evade immunity but also into the many facets of endogenous MIF in a broader context.

Acknowledgments—We are grateful to D. Guiliano for providing EST clones, Council for the Central Laboratory of the Research Councils for use of Synchrotron facilities, and J. Dornan, B. Gregory, Y. Harcus, M. Holland, J. Murray, and N. Gomez-Escobar for invaluable assistance. We thank J. Allen, M. Blaxter, and D. Gray for critical comments on the paper.

REFERENCES

1. Ploegh, H. L. (1998) *Science* **280,** 248–253
2. Alcami, A., and Koszinowski, U. H. (2000) *Immunol. Today* **21,** 447–455
3. Blaxter, M. L., Aslett, M., Guiliano, D., Daub, J., and The Filarial Genome Project. (1999) *Parasitology* **118,** S39–S51
4. Pastrana, D. V., Raghavan, N., FitzGerald, P., Eisinger, S. W., Metz, C., Bucala, R., Schleimer, R. P., Bickel, C., and Scott, A. L. (1998) *Infect. Immun.* **66,** 5955–5963
5. Gomez-Escobar, N., Gregory, W. F., and Maizels, R. M. (2000) *Infect. Immun.* **68,** 6402–6410
6. Michael, E., Bundy, D. A. P., and Grenfell, B. T. (1996) *Parasitology* **112,** 409–428
7. Liu, S., Tobias, R., McClure, S., Styba, G., Shi, Q., and Jackowski, G. (1997) *Clin. Biochem.* **30,** 455–463
8. Mozetic-Francky, B., Cotic, V., Ritonja, A., Zerovnik, E., and Francky, A. (1997) *Protein Expression Purif.* **9,** 115–124
9. Gregory, W. F., Blaxter, M. L., and Maizels, R. M. (1997) *Mol. Biochem.*

Parasitol. **87,** 85–95
10. Zang, X. X., Atmadja, A. K., Gray, P., Allen, J. E., Gray, C. A., Lawrence, R. A., Yazdanbakhsh, M., and Maizels, R. M. (2000) *J. Immunol.* **165,** 5161–5169
11. Su, S. B., Gong, W., Gao, J. L., Shen, W., Murphy, P. M., Oppenheim, J. J., and Wang, J. M. (1999) *J. Exp. Med.* **189,** 395–402
12. Otwinowski, Z., and Minor, W. (1997) *Methods Enzymol.* **276,** 307–357
13. Terwilliger, T. C., and Berendzen, J. (1999) *Acta Crystallogr. Sec. D* **55,** 849–861
14. Cowtan, K. (1994) *Protein Crystallography* **31,** 34–38
15. Williams, S. A., Lizotte-Waniewski, M. R., Foster, J., Guiliano, D., Daub, J., Scott, A. L., Slatko, B., and Blaxter, M. L. (2000) *Int. J. Parasitol.* **30,** 411–419
16. Tan, T. H., Edgerton, S. A., Kumari, R., McAlister, M. S., Roe, S. M., Nagl, S., Pearl, L. H., Selkirk, M. E., Bianco, A. E., Totty, N. F., Engwerda, C., Gray, C. A., Meyer, D. J., and Rowe, S. M. (2001) *Biochem. J.* **357,** 373–383
17. Marson, A. L., Tarr, D. E. K., and Scott, A. L. (2001) *Gene* (*Amst.*) **278,** 53–62
18. Maizels, R. M., and Lawrence, R. A. (1991) *Parasitol. Today* **7,** 271–276
19. Zang, X. X., Yazdanbakhsh, M., Kiang, H., Kanost, M. R., and Maizels, R. M. (1999) *Blood* **94,** 1418–1428
20. Manoury, B., Gregory, W. F., Maizels, R. M., and Watts, C. (2001) *Curr. Biol.* **11,** 447–451
21. Zang, X., and Maizels, R. M. (2001) *Trends Biochem. Sci.* **26,** 191–197
22. Maizels, R. M., Gomez-Escobar, N., Gregory, W. F., Murray, J., and Zang, X. (2001) *Int. J. Parasitol.* **31,** 889–898
23. Bernhagen, J., Calandra, T., Mitchell, R. A., Martin, S. B., Tracey, K. J., Voelter, W., Manogue, K. R., Cerami, A., and Bucala, R. (1993) *Nature* **365,** 756–759
24. Matsunaga, J., Sinha, D., Pannell, L., Santis, C., Solano, F., Wistow, G. J., and Hearing, V. J. (1999) *J. Biol. Chem.* **274,** 3268–3271
25. Swope, M. D., Sun, H.-W., Blake, P., and Lolis, E. (1998) *EMBO J.* **17,** 3534–3541
26. Pennock, J. L., Wipasa, J., Gordge, M. P., and Meyer, D. J. (1998) *Biochem. J.* **331,** 905–908
27. Kleemann, R., Hausser, A., Geiger, G., Mischke, R., Burger-Kentischer, A., Flieger, O., Johannes, F. J., Roger, T., Calandra, T., Kapurniotu, A., Grell, M., Finkelmeier, D., Brunner, H., and Bernhagen, J. (2000) *Nature* **408,** 211–216
28. Goerdt, S., and Orfanos, C. E. (1999) *Immunity* **10,** 137–142
29. Loke, P., MacDonald, A. S., Robb, A., Maizels, R. M., and Allen, J. E. (2000) *Eur. J. Immunol.* **30,** 2669–2678
30. Donnelly, S. C., Haslett, C., Reid, P. T., Grant, I. S., Wallace, W. A. H., Metz, C. N., Bruce, L. J., and Bucala, R. (1997) *Nat. Med.* **3,** 320–323
31. Sun, H.-W., Bernhagen, J., Bucala, R., and Lolis, E. (1996) *Proc. Natl. Acad. Sci. U. S. A.* **93,** 5191–5196
32. Suzuki, M., Sugimoto, H., Nakagawa, A., Tanaka, I., Nishihira, J., and Sakai, M. (1996) *Nat. Struct. Biol.* **3,** 259–266
33. Lubetsky, J. B., Swope, M., Dealwis, C., Blake, P., and Lolis, E. (1999) *Biochemistry* **38,** 7346–7354
34. Taylor, A. B., Johnson, W. H., Jr., Czerwinski, R. M., Li, H. S., Hackert, M. L., and Whitman, C. P. (1999) *Biochemistry* **38,** 7444–7452
35. Maizels, R. M., Bundy, D. A. P., Selkirk, M. E., Smith, D. F., and Anderson, R. M. (1993) *Nature* **365,** 797–805
36. King, C. L., Mahanty, S., Kumaraswami, V., Abrams, J. S., Regunathan, J., Jayaraman, K., Ottesen, E. A., and Nutman, T. B. (1993) *J. Clin. Invest.* **92,** 1667–1673
37. Metz, C. N., and Bucala, R. (1997) *Adv. Immunol.* **66,** 197–223
38. Bucala, R. (2000) *Nature* **408,** 146–147
39. Roger, T., David, J., Glauser, M. P., and Calandra, T. (2001) *Nature* **414,** 920–924
40. Bloom, B. R., and Bennett, B. (1966) *Science* **153,** 80–82
41. David, J. R. (1966) *Proc. Natl. Acad. Sci. U. S. A.* **56,** 72–77
42. Galat, A., Riviere, S., and Bouet, F. (1993) *FEBS Lett.* **319,** 233–236
43. Weiser, W. Y., Temple, P. A., Witek-Giannotti, J. S., Remold, H. G., Clark, S. C., and David, J. R. (1989) *Proc. Natl. Acad. Sci. U. S. A.* **86,** 7522–7526
44. Rosengren, E., Aman, P., Thelin, S., Hansson, C., Ahlfors, S., Bjork, P., Jacobsson, L., and Rorsman, H. (1997) *FEBS Lett.* **417,** 85–88
45. Bozza, M., Satoskar, A. R., Lin, G., Lu, B., Humbles, A. A., Gerard, C., and David, J. R. (1999) *J. Exp. Med.* **189,** 341–346
46. Calandra, T., Echtenacher, B., Le Roy, D., Pugin, J., Metz, C. N., Hultner, L., Heumann, D., Mannel, D., Bucala, R., and Glauser, M. P. (2000) *Nat. Med.* **6,** 164–170
47. de Jong, Y. P., Abadia-Molina, A. C., Satoskar, A. R., Clarke, K., Rietdijk, S. T., Faubion, W. A., Mizoguchi, E., Metz, C. N., Alsahli, M., ten Hove, T., Keates, A. C., Lubetsky, J. B., Farrell, R. J., Michetti, P., van Deventer, S. J., Lolis, E., David, J. R., Bhan, A. K., Terhorst, C., and Sahli, M. A. (2001) *Nat. Immunol.* **2,** 1061–1066
48. Maizels, R. M., Sartono, E., Kurniawan, A., Selkirk, M. E., Partono, F., and Yazdanbakhsh, M. (1995) *Parasitol. Today* **11,** 50–56
49. Lawrence, R. A. (1996) *Parasitol. Today* **12,** 267–271
50. MacDonald, A. S., Maizels, R. M., Lawrence, R. A., Dransfield, I., and Allen, J. E. (1998) *J. Immunol.* **160,** 4124–4132
51. Falcone, F. H., Loke, P., Zang, X., MacDonald, A. S., Maizels, R. M., and Allen, J. E. (2001) *J. Immunol.* **167,** 5348–5354
52. Schönemeyer, A., Lucius, R., Sonnenburg, B., Brattig, N., Sabat, R., Schilling, K., Bradley, J., and Hartmann, S. (2001) *J. Immunol.* **167,** 3207–3215
53. Tang, L., Smith, V. P., Gounaris, K., and Selkirk, M. E. (1996) *Exp. Parasitol.* **82,** 329–332
54. LoVerde, P. T. (1998) *Parasitol. Today* **14,** 284–289
55. Wray, G. A., Levinton, J. S., and Shapiro, L. H. (1996) *Science* **274,** 568–573
56. Mitchell, R. A., and Bucala, R. (2000) *Semin. Cancer Biol.* **10,** 359–366